Int. J. Electrochem. Sci., 8 **(2013)** 3687 - 3695

International Journal of
ELECTROCHEMICAL
SCIENCE
www.electrochemsci.org

Effects of Microporous Layer on PBI-based Proton Exchange Membrane Fuel Cell Performance

Chun-Ting Liu, Min-Hsing Chang[*]

Department of Mechanical Engineering, Tatung University, Taipei 104, Taiwan
[*]E-mail: mhchang@ttu.edu.tw

Received: 17 January 2013 / *Accepted:* 9 February 2013 / *Published:* 1 March 2013

This study investigates the influence of microporous layer (MPL) on the performance of a high-temperature proton exchange membrane fuel cell utilizing a phosphoric-acid-doped polybenzimidazole (PBI) electrolyte. The effects of MPL compositions including polytetrafluorethylene (PTFE) and carbon black are considered. Under the same catalyst loading, phosphoric acid doping level, and operation conditions, the fuel cell performance is measured to evaluate the importance of MPL and determine the optimal PTFE content and carbon loading. The method of electrochemical impedance spectroscopy is employed to characterize the variations in the ohmic resistance and polarization losses within the cell. The results show that both the PTFE content and carbon loading in the MPL may affect the cell performance significantly. The MPL with a PTFE content of 40 wt% and carbon loading of 1.0 mg cm^{-2} is found to give the optimal cell performance.

Keywords: Polybenzimidazole; Microporous layer; Polytetrafluorethylene; Carbon loading.

1. INTRODUCTION

Polybenzimidazole (PBI) based high-temperature proton exchange membrane (PEM) fuel cells have advanced rapidly in the past decade owing to their several attractive advantages. Traditional PEM fuel cells that use Nafion® or a similar material as an electrolyte membrane must be hydrated to maintain proton conduction. This condition restricts the operation temperature to less than 90°C and may result in serious problems, for example, the CO poisonous phenomenon of the catalyst layer and the occurrence of flooding on the cathode side. In contrast, PEM fuel cells that employ a polybenzimidazole (PBI) membrane can operate at higher temperatures (120°C~200°C); thus, can enhance the CO tolerance of the catalyst and eliminate the problem of complicated water management. Numerous experimental studies on PBI-based PEM fuel cells have been conducted to investigate their characteristics [1-21]. However, most of the studies used commercially available membrane electrode

assemblies (MEAs) [3-7] or prepared MEAs with a fixed polytetrafluorethylene (PTFE) content and carbon loading in the microporous layer (MPL) [8-19]. The influences of the PTFE content of the gas diffusion layer (GDL) and the PTFE and carbon loadings in the MPL on the cell performance are usually ignored. The gas diffusion media generally consist of a layer of substrate such as carbon paper or cloth with an MPL coating on the surface facing the proton conduction membrane. As pointed out by Seland et al. [10], the carbon paper or cloth is generally wet-proofed by incorporating PTFE in its fiber structure. The substrate is wet-proofed to prevent it from getting soaked during the spraying procedure in the MPL coating process and reduce the penetration of carbon powder into the substrate. The coating of MPL on the substrate surface before the deposition of a catalyst layer has been found to be beneficial because the MPL coating can prevent the catalyst particles from penetrating into the substrate and ensure a good electronic bonding between the substrate and the catalyst layer. The MPL is generally made up of PTFE and carbon powder; PTFE is used to enhance the bonding between the MPL and the substrate rather than enhancing the water management in a PBI-based high-temperature fuel cell. Lobata et al. [20] first considered the influence of the PTFE loading in the GDL on the cell performance. They used commercial Toray graphite paper as the GDL and found that the lower the PTFE content, the better was the cell performance. Accordingly, they suggested that the PTFE content in the carbon paper should be as low as possible. Their results showed that carbon paper loaded with 10% PTFE might provide good mechanical properties while causing only a slight degradation in the cell performance. They further considered the effect of carbon loading in the MPL [21] and found that for a GDL made of carbon paper, the optimal carbon loading is 2 mg cm^{-2} for both the anode and the cathode sides. So far very few studies have performed related investigations. Motivated by this, in the present study, we performed systematic measurements to determine the effect of the PTFE content and carbon loading in the MPL on the performance of a PBI-based PEM fuel cell. The MEA was fabricated using a commercial PBI membrane with carbon cloths (used as the GDLs). The GDL surface was coated on one side with MPL having different PTFE contents and carbon loadings. Accordingly, the optimal composition of the MPL could be evaluated by testing the variation in the cell performance.

2. EXPERIMENTAL

In the fuel cell structure, the central MEA consists of a PBI membrane and two GDLs made of carbon cloth. Each GDL has a coating of MPL and a catalyst layer on the surface facing the membrane to form the gas diffusion electrode (GDE). Teflon gaskets are installed around the MEA to prevent possible gas leakage. A serpentine flow channel is machined on each graphite plate to supply reactant gases. The reactant gases enter and leave the fuel cell through the inlets and outlets, respectively, on the end plates and four Teflon tubes are used to connect the flow channels between the end plates and graphite plates. All the components are bolted together to form a single cell with a torque $40\ \mathrm{kgf \cdot cm}$ applied on each bolt. During testing of the fuel cell performance, the entire cell is placed in an electrical heating jacket to maintain uniform temperature. The cell temperature is kept constant at $180^{\circ}\mathrm{C}$ in all the experiments.

The PBI membrane used in these experiments is made of Advent® (series number GSM006077); the membrane thickness is 50 μm before the doping of phosphoric acid. For the preparation of the MEA, the PBI membrane was first immersed in an 85 wt% phosphoric acid bath at 60 °C to achieve proton conduction. The doping level was estimated from the change in membrane weight before and after doping, and it was controlled to approximately 6.7 molecules of acid per repeat unit of PBI. To prepare the GDEs, a GDL made of carbon cloth (E-TEK Inc., B1ASWP Designation A, 400 μm thick, 30% wet-proofed) was used as the substrate; then, it was deposited by spraying an MPL on the surface facing the PBI membrane. The MPL consists of Vulcan XC-72R carbon black and PTFE. In order to determine the optimal composition of the MPL, the loadings of carbon powder and PTFE within the MPL were adjusted within the ranges of 0.5~2.0 mg cm^{-2} and 0% ~ 60 wt%, respectively. After coating the MPL, the catalyst layer was deposited onto the MPL to form the GDE. The catalyst ink was prepared from Pt/C powder (20 wt% Pt on Vulcan XC-72, E-TEK Inc.), PBI solution (5 wt% in *N*,*N*-dimethylacetamide (DMAc)), and DMAc as solvent. The platinum catalyst loading was 1.0 mg cm^{-2}. To remove DMAc, the GDE was dried in an air circulation oven after the deposition of catalyst layer and then sintered at 190 °C for 2 h. Next, the GDE was wetted with a 10 wt% phosphoric acid solution for one day in order to absorb the acid. Finally, the doped PBI membrane was sandwiched between the two GDEs to form the MEA. The reaction area on the MEA was 2 cm × 2 cm. The same GDEs, on both the anode and the cathode sides, were used in all the experiments.

The experimental measurements focus on determining the effect of the MPL composition on the fuel cell performance, and the optimal composition of the MPL. Accordingly, the cell performance was measured under different loadings of carbon black and PTFE contents. A Hephas® P-300 fuel cell test station was employed to measure the cell performance and obtain polarization curves. Pure hydrogen and compressed air were used as the fuel and the oxidant, respectively. The flow rates of hydrogen and air were controlled by mass flow controllers (MFCs) fixed at 150 sccm and 350 sccm, respectively. Before measuring the polarization curve, the MEA was first conditioned at a fixed potential of 0.6 V for 24 h to ensure that the cell performance is stabilized and produces steady current. The polarization curves were obtained by scanning the cell potential from an open circuit voltage (OCV) to 0.3 V and then recording the resulting current densities. The Electrochemical impedance spectroscopy (EIS) measurements were also performed to characterize the contributions to the cell resistance. A frequency response analyzer (FRA) module coupled with an Autolab PGSTAT 302N potentiostat was employed in the EIS measurements. The impedance spectra were recorded by sweeping frequencies over the range of 10 mHz to 10 kHz with the amplitude of the AC current held at 5% of that of the DC current. The obtained spectra were further analyzed by an equivalent circuit to investigate the characteristics of the cell performance.

3. RESULTS AND DISCUSSION

The tests were divided into two parts. First, we considered the effect of different carbon loadings in the MPL while keeping the PTFE content constant in the tests. The optimal carbon loading

was determined by evaluating the variation in the polarization curves at different carbon loadings. Second, the influence of the different PTFE contents in the MPL was measured while keeping the carbon loading constant in the tests. Accordingly, the optimal composition of the MPL was determined.

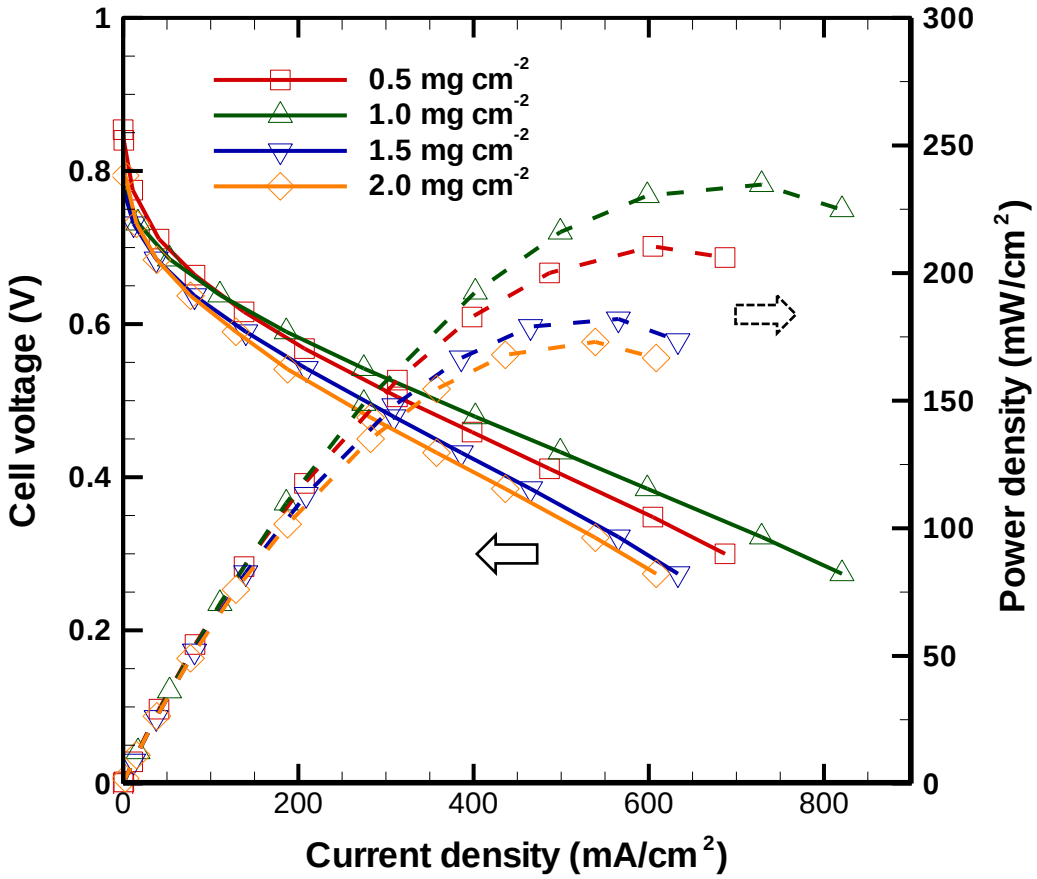

Figure 1. Polarization and corresponding power density curves at different carbon loadings in the MPL. The PTFE content is fixed at 40 wt%.

The polarization curves at different carbon loadings with a 40% PTFE content in the MPL are shown in Fig. 1. Clearly, the variation of carbon loading in the MPL significantly affects the cell performance. With an increase in the carbon loading from 0.5 to 1.0 mg cm^{-2}, the limiting current density increased from 690 to 820 mA cm^{-2} and the corresponding peak power density increased from 210 to 240 mW cm^{-2}. However, once the carbon loading was increased beyond 1.5 mg cm^{-2}, the cell performance degraded significantly, and it was worse than that at the initial carbon loading of 0.5 mg cm^{-2}. The limiting current density and peak power density reduced to 630 mA cm^{-2} and 180 mW cm^{-2}, respectively. The cell performance degraded continuously with increasing carbon loading to 2.0 mg cm^{-2}. Therefore, the carbon loading of 1.0 mg cm^{-2} in the MPL was found to give the best cell performance. It is noteworthy that the variation in OCV was quite small in these cases, indicating that the amount of fuel crossover and the internal current within the cell are insensitive to the change of carbon loading in the MPL.

EIS was also used to investigate the cell performance and provide further understanding of the effect of carbon loading. Impedance spectra at a typical carbon loading of 0.5 mg cm^{-2} as a function of the current density are illustrated in Fig. 2.

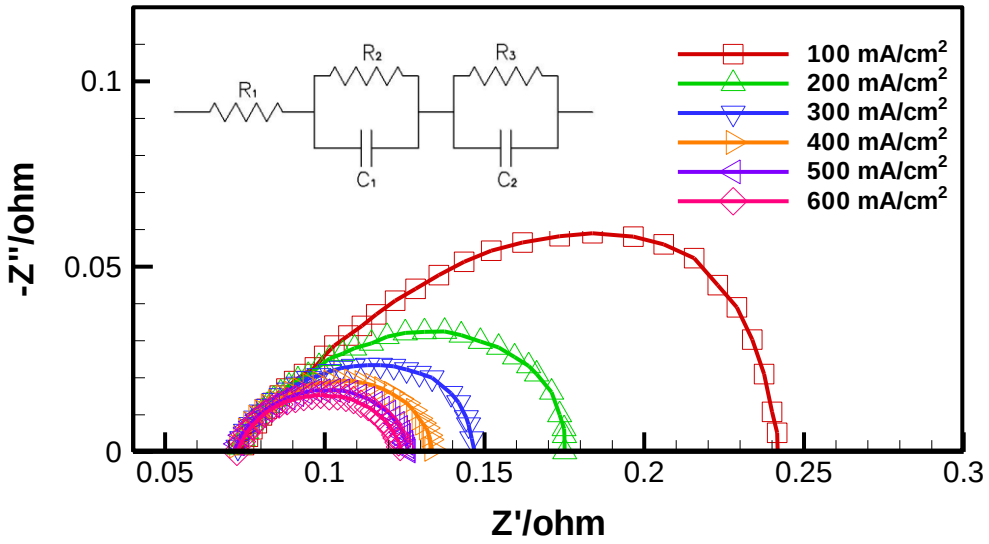

Figure 2. Impedance spectra at different current densities for a typical case of carbon loading of 0.5 mg cm^{-2} in the MPL.

The equivalent circuit embedded in Fig. 2 was used to fit the impedance data. It consists of an ohmic resistance R_1, in series with a first resistance (R_2)/constant phase element (C_1), and then a second resistance (R_3)/constant phase element (C_2). The intercept of the horizontal real axis of the impedance spectrum at the left end of the arc represents the ohmic resistance of the fuel cell, R_1. In general, two distinct arcs can be observed for a high temperature PBI-based fuel cell. The left depressed arc in the high-frequency region is usually quite small which is attributed to the coupling of the distributed ionic resistance and capacitance in the catalyst layer [19]. The depressed high-frequency loop can be detected at different current densities and its variation is very limited with changing current densities. It has been reported that many factors may influence the smaller high-frequency loop, such as the MEA structure, high-frequency relaxation to the distributed resistance effects in the catalyst layer, or the contact capacitance in the electrode structure [22]. However, this high-frequency feature is generally ignored [22] and the spectra can still be analyzed to highlight the characteristics of the electrode process. The right arc in the low-frequency region is ascribed to the polarization process of the cathode which includes both charge transfer and diffusive losses. In the equivalent circuit, the resistances R_2 and R_3 correspond to the high-frequency and low-frequency arcs, respectively. Therefore, the effect of R_2 is generally ignored. As demonstrated in Fig. 2, the ohmic resistance R_1 is almost invariable with increasing current density, and the diameter of the low-frequency arc reduces gradually. The ohmic (R_1) and polarization (R_3) resistances at different carbon

loadings in the MPL are given in Table 1 at the operating current density of 600 $mA\,cm^{-2}$. It can be observed that the variation in R_1 with the carbon loading in MPL is limited. The ohmic resistance is mainly due to the membrane resistance and the resistance arising from the electrode structure. Its value depends on the doping level of the acid in the membrane as well as the composition in the electrodes.

Table 1. Ohmic (R_1) and polarization (R_3) resistances at different carbon loadings in MPL.

Carbon loading (mg/cm^2)	$R_1\,(\Omega\cdot cm^2)$	$R_3\,(\Omega\cdot cm^2)$
0.5	0.290	0.208
1.0	0.198	0.253
1.5	0.212	0.329
2.0	0.252	0.556

The membrane resistance is supposed to be constant in all the cases with the same doping level of phosphoric acid [3]. Thus, the magnitude of R_1 changes slightly with the variation of carbon loading in the MPL since the coating of MPL could affect the condition of electronic bonding between the gas diffusion medium and the catalyst layer. The results show that the minimum ohmic resistance was obtained with the carbon loading of 1.0 $mg\,cm^{-2}$. However, the polarization resistance increases gradually with the carbon loading and rises rapidly when the carbon loading is over 1.0 $mg\,cm^{-2}$. This indicates that an increase of carbon loading in MPL could lower the kinetic and mass transfer conditions in the electrode. Higher carbon loading may reduce the effectiveness of the catalyst layer coated on the substrate. Combining the effects of both R_1 and R_3, the result indicates that the enhancement in the cell performance from carbon loading 0.5 to 1.0 $mg\,cm^{-2}$ is mainly due to the reduction in the ohmic resistance. Once the carbon loading increases further to 1.5 $mg\,cm^{-2}$ or more, the polarization resistance becomes dominant and causes the cell performance to degrade significantly.

We further considered the effect of the PTFE content, while keeping the carbon loading fixed to a value of 1.0 $mg\,cm^{-2}$ according to the results of carbon loading tests. The polarization curves and the corresponding power densities at different PTFE contents in the MPL are shown in Fig. 3. It can be seen that the influence of the PTFE content is more pronounced than that of carbon loading in the MPL. The peak power density increases significantly from approximately 98 $mW\,cm^{-2}$ to 240 $mW\,cm^{-2}$ when the PTFE content increases from 0% to 40%. Once the PTFE content exceeds 40%, the cell performance begins to degrade significantly. According to this result and Fig. 1, we could conclude that the optimal composition of the MPL should be carbon loading of 1.0 $mg\,cm^{-2}$ and PTFE content of 40%. The result shown in Fig. 3 also indicates that the PTFE content in the MPL is a critical factor that may affect the cell performance profoundly. In general, low-temperature PEM fuel cells use a Nafion® membrane as an electrolyte, and their gas diffusion media usually contain PTFE as a hydrophobic agent to improve their water transport performance, especially on the cathode side [1]. Hence, the flooding phenomenon can be avoided and the water content of the membrane can be controlled to maintain appropriate proton conductivity.

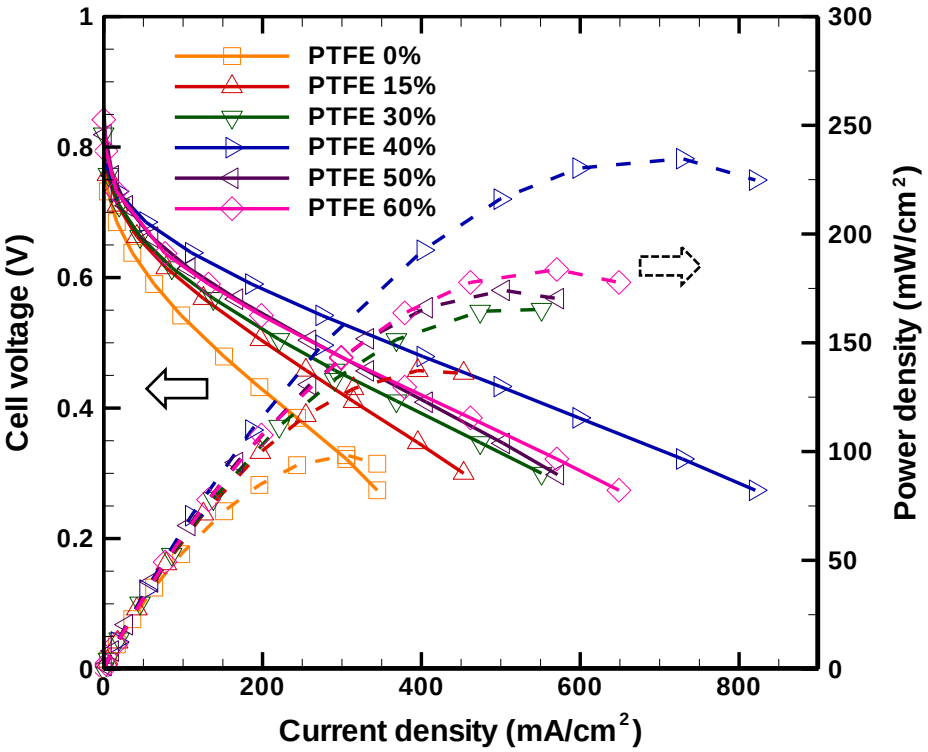

Figure 3. Polarization amd corresponding power density curves at different PTFE contents in the MPL. The carbon loading is fixed to 1.0 mg cm^{-2}.

However, the influence of the PTFE content of the high-temperature PBI-based PEM fuel cell is usually ignored as the operating temperature is generally over 120 °C, and thus, the flooding problem can be resolved naturally.

Table 2. Ohmic (R_1) and polarization (R_3) resistances at different PTFE contents in MPL.

PTFE content (wt %)	R_1 ($\Omega \cdot cm^2$)	R_3 ($\Omega \cdot cm^2$)
15	0.237	0.556
30	0.194	0.394
40	0.202	0.258
50	0.227	0.302
60	0.233	0.311

The present result shows that an appropriate PTFE content of the MPL is still quite important for PBI-based PEM fuel cells. The main reason for this can be explored further by examining the impedance spectra. Figure 4 shows the EIS results at different current densities for the typical case with PTFE content of 40% in the MPL. Similar to the spectra shown in Fig. 2, a depressed high-frequency arc and a significant low-frequency arc were observed in each case, which indicates that the

polarization resistance is still the dominant mechanism. Using the same technique of equivalent circuit analysis, we can obtain the variations in the ohmic resistance and polarization resistance with the PTFE content in MPL at an assigned current density; the results are shown in Table 2 at the operating current density of 400 $mA\,cm^{-2}$.

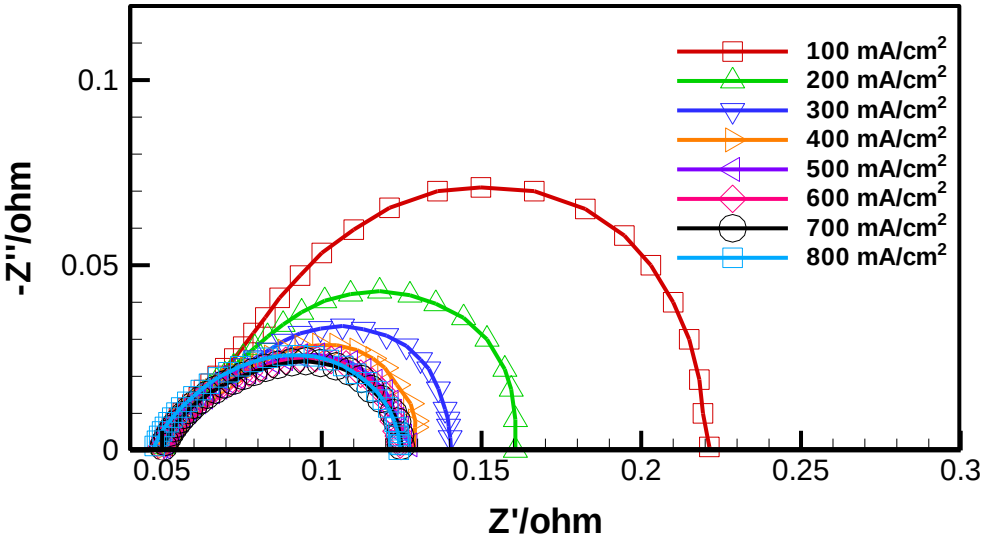

Figure 4. Impedance spectra at different current densities for a typical case of PTFE content of 40 wt% in the MPL.

It can be observed that the ohmic resistance has a minimum at the case of 30% PTFE content and then increases slightly with increasing PTFE content. Note that the difference in R_1 between the cases of 30% and 40% is quite limited. The polarization resistance R_3 is relatively larger at 15% PTFE content. It appears to decrease rapidly with increasing PTFE content, reaches a minimum at 40%, and then increases slowly with PTFE content. This result indicates that the PTFE content in the MPL may affect the reaction kinetics and gas diffusion condition in the electrode significantly and should be a dominant factor in the determination of cell performance. An appropriate PTFE content may enhance the effectiveness of the catalyst layer and thus reduce the corresponding polarization resistance. The overall effect of R_1 and R_3 shows that the case of 40% PTFE content in the MPL could give the optimal cell performance. An increase in the PTFE content beyond 40% may slightly enhance both the ohmic and polarization resistances and thus causes the degradation of the cell performance.

4. CONCLUSIONS

In this study, the effects of carbon loading and PTFE content of the MPL on the performance of a PBI-based high-temperature PEM fuel cell were evaluated experimentally. The purpose of this evaluation was to determine the importance of the MPL as a factor affecting the cell performance and to determine the optimal composition of the MPL by measuring the cell performance at different carbon loadings and PTFE contents of the MPL. The results show that an appropriate composition of

the MPL is quite important in achieving the optimal performance of a PBI-based fuel cell. The optimal composition of the MPL is found to be a carbon loading of 1.0 $mg\,cm^{-2}$ with PTFE content of 40%. The cell performance is more sensitive to the variation of the PTFE content; furthermore, the EIS results show that the polarization resistance in a PBI-based high-temperature fuel cell can be influenced significantly by the PTFE content of the MPL. Further studies focusing on the effect of different carbon powders and hydrophobic agents in the MPL will be interesting and necessary to enhance the performance of a PBI-based high-temperature fuel cell system.

ACKNOWLEDGMENTS
The authors gratefully acknowledge the financial support from National Science Council of Taiwan through the grant NSC 97-2221-E-036-036.

References

1. Y. L. Ma, J. S. Wainright, M. H. Litt, R. F. Savinell, *J. Electrochem. Soc.*, 151 (2004) A8-A16.
2. R. He, Q. Li, A. Bach, J. O. Jensen, N. J. Bjerrum, *J. Membrane Sci*., 277 (2006) 38-45.
3. A.R. Korsgaard, R. Reshauge, M. P. Nielsen, M. Bang, S. K. Kar, *J. Power Sources*, 162 (2006) 239-245.
4. N. H. Jalani, M. Ramani, K. Ohlsson, S. Buelte, G. Pacifico, R. Pollard, R. Staudt, R. Datta, *J. Power Sources*, 160 (2006) 1096-1103.
5. Y. Tang, J. Zhang, C. Song, J. Zhang, *Electrochem. Solid-state Letts.*, 10 (2007) B142-B146.
6. J. Zhang, Y. Tang, C. Song, J. Zhang, *J. Power Sources*, 172 (2007) 163-171.
7. C. Y. Chen, W. H. Lai, *J. Power Sources*, 195 (2010) 7152-7159.
8. J. Hu, H. Zhang, Y. Zhai, G. Liu, J. Hu, B. Yi, *Electrochim. Acta* 52 (2006) 394-401.
9. J. Hu, H. Zhang, Y. Zhai, G. Liu, B. Yi, *Int. J. Hydrogen Energy*, 31 (2006) 1855-1862.
10. F. Seland, T. Berning, B. Borresen, R. Tunold, *J. Power Sources*, 160 (2006) 27-36.
11. G. Liu, H. Zhang, J. Hu, Y. Zhai, D. Xu, Z. Shao, *J. Power Sources*, 162 (2006) 547-552.
12. Y. Zhai, H. Zhang, G. Liu, J. Hu, B. Yi, *J. Electrochem. Soc.*, 154 (2007) B72-B76.
13. K. Scott, S. Pilditch, M. Mamlouk, *J. Appl. Electrochem.*, 37 (2007) 1245-1259.
14. 14 O. E. Kongstein, T. Berning, B. Borresen, F. Seland, R. Tunold, *Energy*, 32 (2007) 418-422.
15. J. Lobato, P. Canizares, M. A. Rodrigo, J. J. Linares, *Electrochim. Acta*, 52 (2007) 3910-3920.
16. S. Yu, L. Xiao, B. C. Benicewicz, *Fuel Cells*, 8 (2008) 165-174.
17. E. U. Ubong, Z. Shi, Z. Wang, *J. Electrochem. Soc*., 156 (2009) B1276-B1282.
18. M. Mamlouk, K. Scott, *Int. J. Hydrogen Energy*, 35 (2010) 784-793.
19. J. Lobato, P. Canizares, M. A. Rodrigo, J. J. Linares, F. J. Pinar, *Int. J. Hydrogen Energy*, 35 (2010) 1347-1355.
20. J. Lobato, P. Canizares, M. A. Rodrigo, C. Ruiz-Lopez, J. J. Linares, *J. Appl. Electrochem*., 38 (2008) 793-802.
21. J. Lobato, P. Canizares, M. A. Rodrigo, D. Ubeda, F. J. Pinar, J. J. Linares, *Fuel Cells*, 10 (2010) 770-777.
22. X. Yuan, J. C. Sun, M. Blanco, H. Wang, J. Zhang, D. P. Wilkinson, *J. Power Sources*, 161 (2006) 920-928.